RSC Advances

PAPER

View Article Online
View Journal | View Issue

Cite this: *RSC Adv.*, 2021, **11**, 26883

Evaluation of P-bridged biaryl phosphine ligands in palladium-catalysed Suzuki–Miyaura cross-coupling reactions†‡

Jairus L. Lamola, [a] Paseka T. Moshapo,[a] Cedric W. Holzapfel§[a] and Munaka Christopher Maumela*[ab]

Received 25th June 2021
Accepted 18th July 2021

DOI: 10.1039/d1ra04947j

rsc.li/rsc-advances

A family of biaryl phosphacyclic ligands derived from phobane and phosphatrioxa-adamantane frameworks is described. The rigid biaryl phosphacycles are efficient for Suzuki–Miyaura cross-coupling of aryl bromides and chlorides. In particular, coupling reactions of the challenging sterically hindered and heterocyclic substrates were viable at room temperature.

Introduction

For the past three decades, palladium-catalysed cross-coupling reactions have revolutionised organic synthesis by providing easy and rapid access to compounds of varying levels of structural complexity.[1a,b] Among these is the Suzuki–Miyaura reaction, which has been identified as one of the most versatile methods for carbon–carbon (C–C) bond formation and is pivotal to the synthesis of biaryl intermediates and building blocks for the fine chemical industry.[2a,b] Since its inception, the Suzuki–Miyaura reaction has received a great deal of attention in various fields of chemistry and has advanced significantly. The use of air stable dialkylbiaryl phosphines (Fig. 1) developed by the Buchwald's research group has resulted in a remarkable breakthrough in cross-coupling reactions. For example, Suzuki–Miyaura reaction based on dialkylbiaryl phosphines has been successfully used in the formation of C–C bonds in medicinal chemistry;[3a] material science;[3b] process chemistry;[3c] and synthesis of heterocycles,[3d] natural products,[3e] and ligands.[3f] Interestingly, Buchwald and other researchers have demonstrated that some of these transformations can be conducted at low catalyst loadings,[4a] room-temperature,[4b] short reaction times,[4c] using green solvents,[4d,e] and deactivated substrates.[4f–h] Other advancements and green approaches that have been demonstrated with dialkylbiaryl phosphines include flow chemistry,[4i,j] solvent-free reaction conditions,[4k] and mechanochemically processes (ball milling).[4l] The effectiveness of the well-known dialkylbiaryl phosphines is believed to arise from the electron-rich and sterically hindered characteristics of the dialkyl substituents on the phosphorus atom.[4m] The robustness and air stability of these classes of phosphines is associated with the biaryl backbone.[4n]

Encouraged by the steric and electron donor properties of relatively air stable[5a–c] phosphines bearing phobane (Phob, particularly [3.3.1] isomer) and phosphatrioxa-adamantane (Cg) moieties described by Pringle,[5d] Otto,[5e] Capretta,[5f] and Lautens,[5g] we report the synthesis and structural features of phosphine ligands containing bicyclic Phob and Cg moieties (Fig. 1). The utility of the biaryl phosphacycles in palladium-catalysed Suzuki–Miyaura reactions of aryl bromides and chlorides is also described.

Results and discussion

Ligand synthesis

Prior to the synthesis of the biarylphobane[3.3.1] systems (**1** and **2**), a separation of a *racemic* of isomers (1*s*,5*s*)-9-phospha-bicyclo

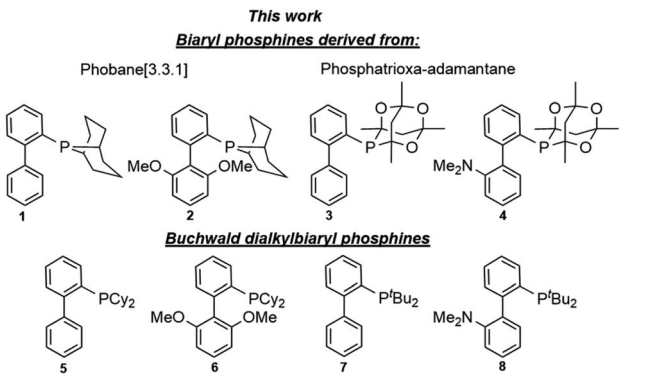

Fig. 1 Biaryl phosphines with bridged bicyclic (**1–4**) and dialkyl (**5–8**) moieties.

[a]*Research Centre for Synthesis and Catalysis, Department of Chemical Sciences University of Johannesburg, Kingsway Campus, Auckland Park 2006, South Africa. E-mail: chris.maumela@sasol.com*

[b]*Sasol (Pty) Ltd, Research and Technology (R & T), 1 Klasie Havenga Rd, Sasolburg 1947, South Africa. E-mail: chris.maumela@sasol.com*

† Dedicated to the memory of Emeritus Professor Cedric Holzapfel (1935–2021). We are eternally grateful for his mentorship and friendship.

‡ Electronic supplementary information (ESI) available: CIFs, crystal data, checkCif reports, NMR (1D & 2D), HRMS & GC-data. CCDC 2051924, 2051881, 2051950 and 2051945. For ESI and crystallographic data in CIF or other electronic format see DOI: 10.1039/d1ra04947j

§ Deceased.

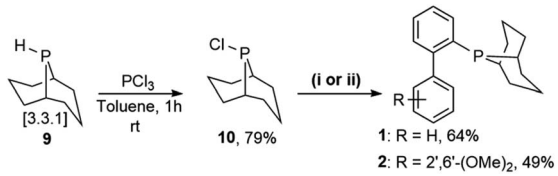

Scheme 1 The synthesis of ligands **1** and **2**, through reaction of phosphine chloride **10** with (i) 2-biphenylmagnesium bromide, CuCl 5 mol%, LiBr 10 mol%, toluene, 110 °C, 12 and Ar; or (ii) (2′,6′-dimethoxy-[1,1′-biphenyl]-2-yl)lithium, THF, −80 °C → RT, 24 h and Ar, respectively.

[3.3.1]nonane (*s*-Phob-H) and (1*R*,6*S*)-9-phospha-bicyclo[4.2.1]nonane (*a*-Phob-H) was conducted. Otto and co-workers[5e] have shown that tertiary phosphines based on *s*-Phob exhibited superior coordinating ability and catalytic potential than the *a*-Phob counterpart. With compound **9** in hand, chlorination of the phosphine by treatment with PCl_3 afforded phobane[3.3.1] chloride **10** in 79% isolated yield (Scheme 1). Lastly, phobane[3.3.1] chloride **10** was reacted with a suitable biaryl backbone to furnish the desired biarylphobane[3.3.1] ligands **1** and **2** in 64% and 49% isolated yields, respectively. The Cg-based systems **3** and **4** were synthesised in a one-step palladium-catalysed C–P cross-coupling reaction of Cg-H with a suitable biaryl bromide, similar to the procedure described by Lautens[5g] and Shekhar.[5h] Ligands **3** and **4** were obtained in 76% and 80% isolated yields, respectively.

Upon isolation, biaryl phosphacycles derived from *s*-Phob and Cg moieties were recrystallised to obtain clear and white crystals, respectively. Through X-ray crystallography, the molecular structures and selected crystal data of the entire ligand library are described (Table 1).

The shorter P–C_{Ar} bond in bridged bicyclic systems **1–4** compared to Buchwald congeners **6** and tetramethyl-^{t}BuXPhos (**11**) (Table 2), was suspected to be a result of the inherent freedom to rotation of the Cy and ^{t}Bu, opposed to the "caged" Phob and Cg moieties.[6a] The C_{Ar}–P–C_{Phob} bond angles of biaryl phosphines **1** and **2** were larger than C_{Ar}–P–C_{Cy} of phosphine **5**, while the C_{Ar}–P–C_{Cg} bond angles of phosphines **3** and **4** were smaller than C_{Ar}–P–$C_{t\text{-}Bu}$ of phosphine **11**, Table 2. There is no general correlation of bond lengths and angles of free ligands to their catalytic potential, in contrast to studies of phosphine–metal complexes.[6b–e] However, studies by Tyler's group[6f] revealed the remarkably short P–M bond and strong σ-donating character of [1,1′-biphenyl-2-yl]dimethylphosphine (MeJPhos) as a manifest of its slightly distorted trigonal pyramid geometry (C_{Ar}–P–C_{Me}, 100.3°). According to Tyler, the slight distortion reduces "front strain", allowing the P lone pair to occupy an sp^3-like orbital which has strong overlap with metal center.[6f] Similarly, Otto and Bungu[6g] found strong σ-donation to be a result of the correlation between short P–C_{Phob} bond lengths (1.809 Å, phobane[3.3.1]-Ph contrary to 1.863 Å, phobane[4.2.1]-Ph) and effective orbital overlap due to less geometry distortion.

The observed magnitudes of the biaryl torsions increase with substituents on the *o*-aryl (bottom ring) (Table 2). The functionalised biaryl phosphacycles **2** and **4** exhibited larger torsions (72.47° and 65.78°) compared to the unsubstituted

Table 2 Selected bond lengths, angles, and torsional angles of phosphines **1–4** and comparison with **6** (ref. 6*h*) and **11** (ref. 6*i*)[a]

Ligand	P–C_{Ar} (Å)	C–P–C_{Ar}[b] (°)	Biaryl torsion angle (°)
1	1.841	104.34, 106.08	52.74
2	1.844	104.27, 107.45	72.47
3	1.839	103.94, 106.00	61.89
4	1.839	103.09, 106.51	65.78
6	1.850	102.96, 103.36	73.79
11	1.875	107.08, 110.65	91.41

[a] The average values were employed for systems with more than one molecule in the asymmetric unit. [b] Bond angle generated between the P-donor atom and its immediate neighbouring carbons ($C_{cyclic/alkyl}$–P–C_{Ar}). The observed trigonal pyramidal geometries for **1–4** correlates to the commonly accepted trigonal pyramidal angle ($90° < \theta < 109.5°$).

Table 1 Selected crystallographic data of the biaryl phosphacycles[a]

Crystal structure			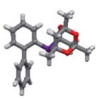	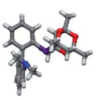
Ligand	**1**	**2**	**3**	**4**
CCDC no.	2051924	2051881	2051950	2051945
Empirical formula	$C_{20}H_{23}P$	$C_{44}H_{54}O_4P_2$	$C_{22}H_{25}O_3P$	$C_{24}H_{30}NO_3P$
Crystal system	Monoclinic	Triclinic	Triclinic	Monoclinic
Space group	*P*2/*n*	$P\bar{1}$	$P\bar{1}$	*C*2/*c*
a/Å	14.554(2)	10.80490(10)	8.0873(7)	23.219(2)
b/Å	7.2220(11)	13.8758(2)	9.4963(9)	8.4649(8)
c/Å	31.176(4)	14.4304(2)	13.1468(12)	24.795(2)
α/°	90	62.5460(10)	92.553(4)	90
β/°	97.878(5)	81.2320(10)	105.035(4)	110.975(2)
γ/°	90	88.0550(10)	95.537(4)	90
Final *R* indexes [$I \geq 2\sigma(I)$]	$R_1 = 0.0413$, $wR_2 = 0.0941$	$R_1 = 0.0344$, $wR_2 = 0.0914$	$R_1 = 0.0446$, $wR_2 = 0.1056$	$R_1 = 0.0358$, $wR_2 = 0.0910$

[a] Full data collection, refinement parameters, and 50% probability ellipsoid plots in ESI.

biaryl phosphacycles **1** (52.74°) and **3** (61.89°), respectively (Table 2). A close correlation was observed between torsions of biaryl phosphines **2** (72.47°) and **5** (73.79°), both bearing 2′,6′-$(OMe)_2$ substituents. Barder and Buchwald[4n] demonstrated the significant role of substituents on the *o*-aryl group, revealing enhanced stability to air and O_2 (at 100 °C) for trisubstituted ligands such as 2-di-*tert*-butylphosphino-2′,4′,6′-triisopropylbiphenyl (^{t}BuXPhos) and 2-(diphenylphosphino)-2′,4′,6′-triisopropylbiphenyl (PhXPhos), without correlations to biaryl torsions. In addition to stability induced by the biaryl backbone, Tyler's group also observed a contribution to steric effects from the MeJPhos biphenyl (torsion 66.8°).[6f]

Catalytic activity

Having successfully synthesised and authenticated the structures of ligands **1–4**, catalytic evaluation commenced by establishing suitable conditions for the coupling of 4-bromotoluene and phenylboronic acid as the model reaction (Table S6, ESI‡). It was established that coupling proceeded in 100% conversion and selectivity towards the desired biaryl product, in the presence of 1 mol% $Pd(OAc)_2$, 2 mol% ligand (**1** and **3**), 3 equiv. KOH dissolved in MeOH (2 M base solution), THF as the solvent for 12 h at room temperature (25 °C). Examining the optimal base in other conventional solvents[7a,b] such as DMA, DMF, and dioxane, afforded lower yields of the desired biaryl product. Similarly, the use of traditional cross-coupling bases K_3PO_4 (ref. 7*c–e*) and KF[7f,g] in THF afforded cross-coupling in diminished yields. Expansion of the optimisation by employing other known bases such as TBAF,[7h] Cs_2CO_3,[7i] and K_2CO_3 (ref. 7*c* and 7*j*) showed inferior results (Table S6, ESI‡).

With the optimal reaction conditions in hand, the scope and generality of this coupling system was investigated (Schemes 2 and 3). Selected well-known dialkylbiaryl phosphine ligands developed by Buchwald were also evaluated in this study for comparison purposes and to gauge the effectiveness of the biaryl phosphacycles. Our early experiments included comparing the catalytic potential of Pd catalyst systems derived from biaryl phosphacycles **1** and **3** to those derived from dialkylbiaryl phosphines **5** and **7** (Scheme 2). Coupling reactions involving (i) monosubstituted **12a–b** and (ii) naphthalene-based **12c–b** aryl bromides were achieved at nearly quantitative yields with catalysts based on ligands **1**, **3**, and **5**, and at moderate yields with ligand **7** (Scheme 2). The significant steric bulk of ligand **7**, as previously quantified by other authors,[7o,p] is suspected to have a negative impact on in this coupling system (Scheme 2).

Distinct catalyst performances were observed from the reactions entailing the synthesis of biaryl products **14f–k** bearing *ortho*-substituent(s) (Scheme 2). In general, these coupling reactions were sensitive to the ligand's steric bulk as demonstrated by the poor catalytic performances of catalysts based on ligands **3** and **7** (**14f–i,k**). It is worth mentioning that the synthesis of the sterically encumbered product **14i** was efficiently achieved by catalysts based on ligand **1**. This is one of

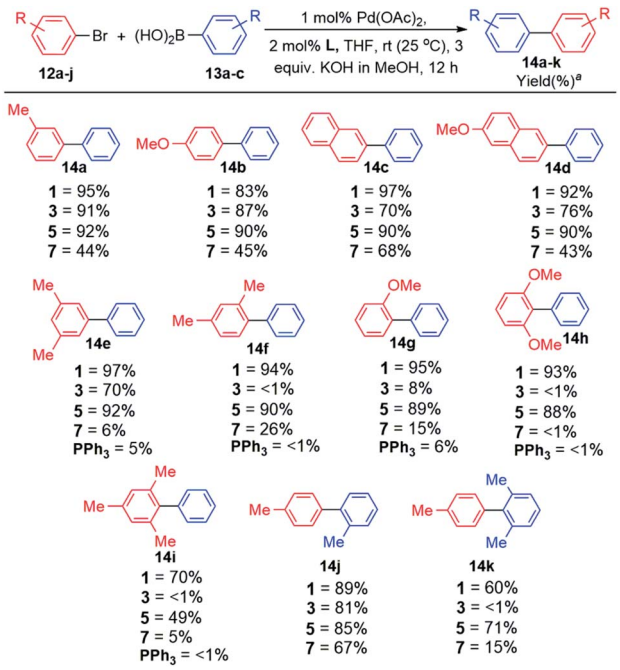

Scheme 2 Substrate scope evaluation. Reaction conditions: ArBr (1 equiv.), $ArB(OH)_2$ (1.5 equiv.), 2 M KOH in MeOH (3 equiv.), $Pd(OAc)_2$ (1 mol%), **L** (2 mol%), THF, Ar, 12 h, rt. [a] Isolated yields from an average of two runs with <5% deviation. GC results included in Tables S5 and S6 (ESI‡).

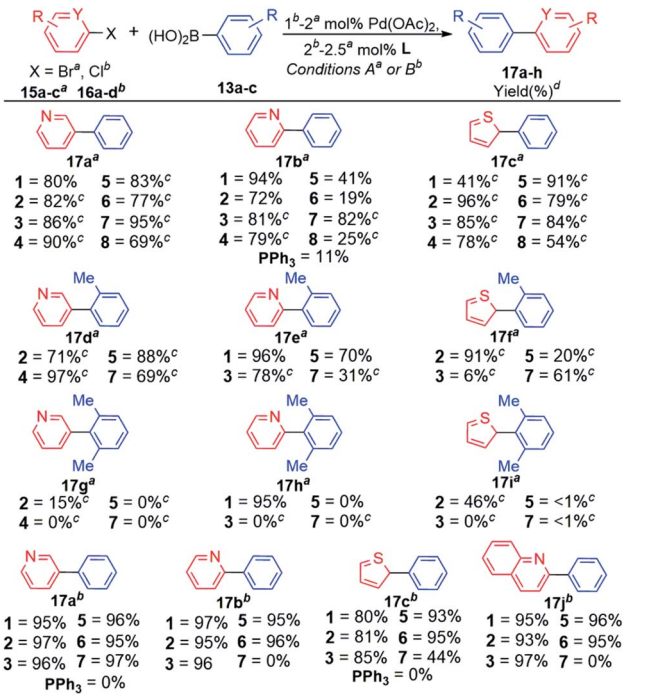

Scheme 3 Substrate scope evaluation. Reaction conditions A: [a]ArBr (1 equiv.), $ArB(OH)_2$ (1.5 equiv.), 2 M KOH in MeOH (3 equiv.), $Pd(OAc)_2$ (2 mol%), **L** (5 mol%), THF, Ar, 24 h, rt. Reaction conditions B: [b]ArCl (1 equiv.), $ArB(OH)_2$ (1.5 equiv.), K_3PO_4 (2 equiv.), $Pd(OAc)_2$ (1 mol%), **L** (2 mol%), toluene, 100 °C, 12 h, Ar. [c]KF as a base. [d] Isolated yields from an average of two runs with <5% deviation. GC results included in Table S5 (ESI‡).

the few reports that demonstrates the room temperature coupling of aryl bromide **12i** since most reports achieved this at elevated temperatures (60–110 °C).[7l–p] Incorporation of bulky substituents on arylboronic acid **13c** impeded coupling reactions using catalysts based on ligands **3** and **7**, containing sterically hindered Cg and ^{t}Bu groups, respectively.

Our attention was then directed to coupling reactions of selected heteroaryl bromides and chlorides (Scheme 3), with a closer look at the most encountered therapeutic scaffolds which includes, (1) pyridine and its derivatives,[8a,b] followed by (2) thiophene.[8c] Early experiments were carried out with the entire ligand scope to gain better understanding of the role of the ligand architecture in these coupling reactions, which are well-known to be less straightforward due to potential catalyst deactivation through undesirable coordination to metal centers.[8d–f]

In general, coupling reactions of heteroaryl bromides **15a–c** with arylboronic acid **13a** were sensitive to the base used, KOH appeared to be ideal for the ligands bearing the less hindered Phob (**1** and **2**) and Cy (**5** and **6**) moieties. The use of KOH with the sterically ligands **3**, **4**, **7**, and **8** favoured side reactions (Table S6, ESI‡). These side reactions were completely suppressed with KF which proved to be the ideal base for the sterically hindered ligands **3**, **4**, **7**, and **8** (Scheme 3). This observation was also noted by Amatore and co-workers.[7g] The authors demonstrated the triple role of fluoride ions in Pd-catalysed Suzuki–Miyaura reaction, which includes: (i) formation of $[ArPdFL_2]$ which is the reactive species for *transmetalation*; (ii) high fluorophilicity of aryl boron moieties which also enhances *transmetalation*; and (iii) promoting reductive elimination *via* the reactive five coordinate $[ArAr'PdFL_2]^-$.[7g] The synthesis of biaryl product **17a**[a] proceeded efficiently only with ligand **1** when KOH was used a base (80% isolated yield, Scheme 3). This coupling appeared to be facile with less hindered ligands[5c,6g] (Table S6, ESI‡). Furthermore, the synthesis of biaryl product **17b**[a] was favourable with KOH as the base for Pd-catalysts derived from biaryl phosphacycles **1–2** and dialkylbiaryl phosphines **5–6**, containing Phob and Cy groups, respectively. Catalyst systems based on ligands **3–4** and **7–8** (containing sterically hindered Cg and ^{t}Bu groups, respectively) were effective with KF as the base. Coupling reactions entailing arylboronic acid **13b** employing the narrowed ligand scope revealed that catalysts based on phobane ligands **1** and **2** exhibited superior performances with average product yields of 86% (**17d–f**[a]). Moderate performances were exhibited by catalysts derived from ligands featuring the Cg, Cy, and ^{t}Bu moieties, with average product yields of 60%, 59%, and 54%, respectively (Scheme 3). Furthermore, catalysts based on these ligands were inactive for the synthesis of biaryl products **17g–i**. Outstanding catalytic performance was achieved in the quantitative formation of biaryl product **17h** (95% isolated yield) using catalysts based on ligand **1**.

Attempts to conduct facile room temperature couplings of aryl chlorides using the established reaction conditions were unsuccessful. As a result, commonly employed reaction conditions were adopted.[3e,7c,d,9a–c] In general, catalysts based on ligands **1–3** consistently exhibited high efficacies in couplings of aryl chlorides **16a–d**, with product yields of 80–97%. Catalysts derived from ligands **5** and **6** also exhibited high product yields of 93–97% for the described products **17a–c,j**[b]. Combination of $Pd(OAc)_2$ and dialkylbiaryl phosphine **7** formed inactive catalysts for Suzuki couplings of 2-chloro-*N*-heterocycles **16b,d** and exhibited diminished efficiency for coupling of heteroaryl chloride **16c**, with a product yield of 44%. Excess steric bulk of ligand **7** appears to impede couplings of the selected 2-chloroheterocycles (Scheme 3). Catalysts based on PPh_3 were inactive in the coupling reactions of heteroaryl chlorides **16a,c**, also observed by Tagata and Nishida.[9d]

Conclusions

In summary, we have developed biaryl phosphines bearing phobane (**1** and **2**) and phosphatrioxa-adamantane (**3** and **4**) frameworks, which formed active catalysts in combination with $Pd(OAc)_2$ for room temperature Suzuki–Miyaura reactions of structurally diverse aryl bromides and boronic acids. These catalyst systems were also effective in coupling reactions of chloro-heteroarenes, with product yields of 88–100%. In general, the catalytic performances of Pd-catalysts based on biaryl phosphacycles ligands were comparable to those based on dialkylbiaryl phosphines with a few examples of distinct catalytic performances. Further application in other Pd-catalysed transformations is in progress.

Experimental section

General methods

All chemicals and anhydrous solvents were purchased from Sigma-Aldrich. All transformations that involve phosphorus derivatives were performed using standard Schlenk line techniques under argon. Secondary bridged phosphines, Phoban-H (m/m in toluene, mixture of isomers [3.3.1] : [4.2.1]) and phosphotrioxa-adamantane (Cg-H) were obtained from Sasol Research & Technology (South Africa). NMR experiments were conducted in $CDCl_3$ solutions using Bruker Ultrashield 400 MHz magnet, an Avance III 400 MHz Console or 500 MHz magnet coupled to an Avance III HD 500 MHz Console. The spectra were calibrated relative to the solvent peaks for ^{1}H and ^{13}C. A SHIMADZU GC-FID was used for the quantification of compounds present in a reaction mixture, using a RTX-1 column ($L = 100$ m, $d = 0.25$ mm) with a film thickness of 0.50 μm. Elemental analysis was conducted on a Flash 2000 Organic Elemental Analyzer, were samples were ran in triplicates and the average was recorded as the final measurement. For accurate mass, samples were analysed on a Waters Synapt G2 quadrupole time-of-flight mass spectrometer, equipped with an ESI probe (electrospray positive mode, 15 V).

Crystallography

X-ray analysis was conducted from two different diffractometers. (i) Single crystal of biaryl phosphacycle **2** was analysed on a Rigaku XtaLAB Synergy R diffractometer, with a rotating-anode X-ray source and a HyPix CCD detector. Data reduction and absorption were carried out using the CrysAlisPro (version 1.171.40.23a) software package.[10a] (ii) Single crystals of biaryl

phosphacycles **1**, **3** and **4** were analysed on a Bruker Apex II DUO diffractometer with a CCD area detector, using a multilayer monochromated Mo-Kα radiation (λ = 0.71073 Å). Data reduction was carried out by means of a standard procedure using the Bruker software package SAINT,[10b] absorption corrections and other systematic errors were accounted for using SADABS.[10c,d] All X-ray diffraction measurements were performed at 100–298 K, using an Oxford Cryogenics Cryostat. All structures were solved by direct methods with SHELXS and SHELXL softwares[10e,f] using the OLEX2 (ref. 10*g*) interface. All H atoms were placed in geometrically idealised positions and constrained to ride on their parent atoms. For data collection and refinement parameters, see (Table S1‡). The X-ray crystallographic coordinates for all structures have been validated through the free online checkCIF platform and later deposited at the Cambridge Crystallographic Data Centre (CCDC), with deposition numbers CCDC: biaryl phosphacycles **1** (2051924), **2** (2051881), **3** (2051950), and **4** (2051945). The attached crystal data folder contains all CIFs, checkCIF reports, and crystal data tables.

Characterisation data

Separation of *s*-Phob-H isomer [3.3.1] by selective oxidation of the *a*-Phob-H isomer [4.2.1].[5d] A methodology reported by Pringle and co-workers was adopted.[5d] A 2 : 1 mixture of Phob-H [3.3.1] : [4.2.1] in toluene (50 cm^3, 158 mmol) was concentrated under argon and reduced pressure to give a colourless oily solid with a very strong order. Aqueous HCl (12 M, 41.5 cm^3) was slowly added over 2 h at 30 °C, under argon. The oily solids were entirely solubilised in the HCl media, in which *s*-Phob-H was selectively protonated. The solution was then cooled to 0 °C and stirred vigorously while H_2O_2 (10.9 cm^3, 30 wt%) was slowly added over 45 min, maintaining the temperature at 0 °C. This was performed to selective oxidize *a*-Phob-H, leaving the protonated *s*-Phob-H unscathed. To ensure full consumption of H_2O_2, the mixture was stirred for another 30 min at room temperature. Degassed hexane (25 cm^3) was added and the mixture was cooled to 0 °C. To this was added an ice-cold solution of NaOH (16 g) in water dropwise. When the addition was completed (*i.e.* neutralization of the protonated *s*-Phob-H), the hexane layer was separated, and the water layer was extracted with degassed hexane (2 × 25 cm^3). The combined organic extracts were dried over $MgSO_4$ and the solvent was removed under argon and reduced pressure to give *s*-Phob-H as a colourless solid (9.25 g, 90%, 97% pure). ^{31}P NMR (202 MHz, $CDCl_3$) δ = −54.17 ppm. NMR data in agreement with Pringle[5d] and Otto's[6g] groups, also see ESI.‡

Synthesis of (1*s*,5*s*)-9-chloro-9-phosphabicyclo[3.3.1]nonane (*s*-Phob-Cl).[5d,6g] A methodology reported by Otto and Bungu was adopted.[6g] PCl_3 (0.32 cm^3, 3.67 mmol) was added dropwise to a degassed toluene solution of *s*-Phob-H (0.62 g, 4.36 mmol) at room temperature under argon. After the addition was complete, the reaction mixture was stirred for 1 h to give a bright yellow solution. The reaction mixture was concentrated under argon and reduced pressure, to give a yellow oily solid, which was extracted repeatedly with degassed diethyl ether (3 × 15 cm^3). The diethyl ether fractions were combined, filtered through a celite plug, and concentrated to give yellow solids of *s*-Phob-Cl (0.51 g, 79%, 90% purity). To improve the purity the solids were either (i) sublimed at 90 °C, 2 mmHg or (ii) dissolved in degassed pentane, passed through a plug of silica/alumina (1 : 1) and concentrated. Both methods improved the purity to >98%. ^{31}P NMR (202 MHz, $CDCl_3$) δ = 89.94 ppm (^{35}Cl isotopomer), 89.90 ppm (^{37}Cl, isotopomer). NMR data in agreement with Pringle[5d] and Otto's[6g] groups, also see ESI.‡

Synthesis of (1*s*,5*s*)-9-([1,1′-biphenyl]-2-yl)-9-phosphabicyclo-[3.3.1]nonane (ligand 1). In a glovebox, CuCl (0.014 g, 0.14 mmol) and LiBr (0.025 g, 0.28 mmol) were transferred to a flame dried Schlenk tube containing degassed toluene (1.00 cm^3). The reaction mixture was stirred at −70 °C, while a 0.50 M solution of 2-biphenylmagnesium bromide in diethyl ether (5.10 cm^3, 2.55 mmol) was added dropwise for 30 minutes. This was followed by the addition of *s*-Phob-Cl (0.50 g, 2.83 mmol) dissolved in degassed toluene (3.00 cm^3). The reaction mixture was allowed to warm-up to room temperature, evacuated and backfilled with argon (10 times) and refluxed (110 °C) for 12 h under argon. The reaction mixture was then cooled to room temperature and diluted with degassed EtOAc (200 cm^3). The solution was poured into a mixture of degassed 28% aqueous NH_4OH (50 cm^3), degassed brine (50 cm^3), and degassed water (50 cm^3), allowed to stir for 10 min. The blue biphasic mixture was separated, and the aqueous layer was kept on the side. The organic layer was washed three times with degassed 28% aqueous NH_4OH (50 cm^3), *i.e.* until all unreacted Cu was removed (transition from blue to clear). All aqueous fractions were combined and further extracted with degassed EtOAc (200 cm^3 × 3), dried over Na_2SO_4 and the solvent was removed under argon. The resulting oil was recrystallised in hot-degassed MeOH (1.00 cm^3), to obtain clear crystalline material which was washed with cold-degassed MeOH (10 cm^3 × 3), affording the title compound (0.53 g, 64%, 100% pure based on ^{31}P NMR). ^{1}H NMR (400 MHz, $CDCl_3$) δ = 7.48 (d, J = 6.8 Hz, 2H$_{(ar)}$), 7.31 (m, 6H$_{(ar)}$), 7.21–7.15 (m, 1H$_{(ar)}$), 2.08–1.90 (m, 4H, P–CH–C$\underline{H}_{2(2eq+2ax)}$, P–CH–C$\underline{H}_{(4ax)}$, P–CH–CH$_2$–C$\underline{H}_{(5eq)}$), 1.88 (bs, 1H, P–CH–C$\underline{H}_{(4eq)}$), 1.85–1.78 (m, 3H, P–CH–C$\underline{H}_{(6eq)}$, P–CH–CH$_2$–C$\underline{H}_{(1eq)}$ and P–CH–C$\underline{H}_{(8eq)}$), 1.60 (bs, 3H, P–C$\underline{H}_{(3ax)}$, P–C$\underline{H}_{(7eq)}$ and P–CH–CH$_2$–C$\underline{H}_{(5ax)}$), 1.49–1.43 (m, 2H, P–CH–C$\underline{H}_{(6ax)}$ and P–CH–C$\underline{H}_{(6ax)}$), 1.29–1.21 (m, 1H, P–CH–CH$_2$–C$\underline{H}_{(1ax)}$). ^{13}C NMR (101 MHz, $CDCl_3$) δ = 145.11 (d, $^1J_{CP}$ = 10.1 Hz, P–C$_{(quat)}$), 142.70 (C$_{(quat)}$), 131.01 (d, J_{CP} = 9.1 Hz, P–CH$_{(ar)}$), 130.32 (CH$_{(ar)}$), 128.46 (d, J_{CP} = 3.0 Hz, P–CH$_{(ar)}$), 128.31 (CH$_{(ar)}$), 127.21 (CH$_{(ar)}$), 126.71 (J_{CP} = 11.1 Hz, P–CH$_{(ar)}$), 31.75 (d, $^2J_{CP}$ = 15.1 Hz, P–CH–$\underline{C}_{(2+4)}$H$_2$), 25.49 (d, $^2J_{CP}$ = 5.0 Hz, P–CH–$\underline{C}_{(6+8)}$H$_2$), 24.54 (d, $^1J_{CP}$ = 12.1 Hz, P–$\underline{C}_{(3+7)}$H), 22.79 (d, $^3J_{CP}$ = 4.0 Hz, P–CH–CH$_2$–$\underline{C}_{(5)}$H$_2$), 21.91 (bs, P–CH–CH$_2$–$\underline{C}_{(1)}$H$_2$). *Peak assignment was achieved by 2D NMR data.* ^{31}P NMR (162 MHz, $CDCl_3$) δ = −19.05. HR-ESI-MS = Calculated m/z = 295.1616 [M + H]$^+$, Found m/z = 295.1624 [M + H]$^+$. Elemental analysis = calculated: C, 81.60%; H, 7.88%; found: C, 81.38%; H, 7.83%.

Synthesis of (1*s*,5*s*)-9-(2′,6′-dimethoxy-[1,1′-biphenyl]-2-yl)-9-phosphabicyclo[3.3.1]nonane (ligand 2). In a glovebox, 2′-bromo-2,6-dimethoxy-1,1′-biphenyl (1.99 g, 6.79 mmol) was transferred to a flame dried Schlenk tube containing super-dry and degassed THF (10 cm^3). The reaction mixture was stirred

−80 °C, while a 2.5 M solution of *n*-butyllithium in hexanes (2.72 cm^3, 6.87 mmol) was added dropwise for 1 h with vigorous stirring. The resulting white reaction mixture was thick and often required hand-assisted stirring. The reaction mixture was warmed to 0 °C, followed by the slow addition of (1*s*,5*s*)-9-chloro-9-phosphabicyclo[3.3.1]nonane (*s*-Phob-Cl, 1.00 g, 5.66 mmol) in super-dry and degassed THF, for 15 min. The reaction mixture was evacuated and backfilled with argon (10 times) and allowed to slowly warm up to room temperature for 24 h, to give a clear yellow solution. This mixture was quenched with saturated and degassed aqueous ammonium chloride (10 cm^3), diluted with degassed ethyl acetate (50 cm^3), and transferred into a separatory funnel. The layers were separated, and the aqueous layer was kept on the side. The organic layer washed with saturated and degassed aqueous ammonium chloride (3 × 10 cm^3) and degassed brine (10 cm^3). All aqueous fractions were extracted with fresh and degassed ethyl acetate (200 cm^3). The organic fractions were dried over Na_2SO_4 and the solvent was removed under argon. The resulting yellow oil was recrystallised in hot-degassed acetone (4.00 cm^3), to obtain clear crystals which were washed with cold-degassed acetone (10 cm^3 × 3), affording the title compound (0.98 g, 49%, 100% pure based on NMR). ^{1}H NMR (500 MHz, $CDCl_3$) δ = 7.36–7.29 (m, 1H, $ArH_{(3)}$), 7.21 (m, 3H, $ArH_{(4-6)}$), 7.09 (bd, J = 7.0 Hz, 1H, $ArH_{(2)}$), 6.51 (d, J = 8.4 Hz, 2H, $ArH_{(1)}$), 3.64 (s, 6H, O<u>Me</u>), 1.94 (m, 6H, P–CH–C<u>H</u>$_{2(2ax+eq)}$, P–CH–CH_2–C<u>H</u>$_{(5ax)}$, P–CH–C<u>H</u>$_{(4eq)}$ and P–CH–C<u>H</u>$_{(6eq)}$ and P–CH–C<u>H</u>$_{(8eq)}$), 1.84–1.74 (m, 2H, P–CH–CH_2–C<u>H</u>$_{(1ax)}$ and P–CH–C<u>H</u>$_{(4ax)}$), 1.60 (bs, 2H, P–C<u>H</u>$_{(3ax)}$ and P–C<u>H</u>$_{(7eq)}$), 1.51 (m, 1H, P–CH–CH_2–C<u>H</u>$_{(5eq)}$), 1.43 (bs, 2H, P–CH–C<u>H</u>$_{(6ax)}$ and P–CH–C<u>H</u>$_{(8ax)}$), 1.28 (m, 1H, P–CH–CH_2–C<u>H</u>$_{(1eq)}$). ^{13}C NMR (126 MHz, $CDCl_3$) δ = 157.89 ($C_{(q1)}$), 139.65 (d, $^1J_{CP}$ = 31.5 Hz, $C_{(q4)}$), 137.36 (d, $^2J_{CP}$ = 11.3 Hz, $C_{(q3)}$), 131.83 ($ArC_{(2)}$), 130.48 (d, $^2J_{CP}$ = 7.7 Hz, $ArC_{(3)}$), 129.06 ($ArC_{(6)}$), 126.67 ($ArC_{(5)}$), 126.04 ($ArC_{(4)}$), 119.47 ($C_{(q2)}$), 103.92 ($Ar_{(C1)}$), 55.83 (O<u>C</u>H_3), 32.02 (d, $^2J_{CP}$ = 15.3 Hz, P–CH–<u>C</u>$_{(2+4)}H_2$), 25.64 (d, $^2J_{CP}$ = 4.2 Hz, P–CH–<u>C</u>$_{(6+8)}H_2$), 25.17 (d, $^1J_{CP}$ = 13.4 Hz, P–<u>C</u>$_{(3+7)}$H), 22.79 (d, $^3J_{CP}$ = 4.6 Hz, P–CH–CH_2–<u>C</u>$_{(5)}H_2$), 22.18 (bs, P–CH–CH_2–<u>C</u>$_{(1)}H_2$). *Peak assignment was achieved by 2D NMR data*. ^{31}P NMR (202 MHz, $CDCl_3$) δ = −16.26. HR-ESI-MS = calculated m/z = 355.1827 $[M + H]^+$, found m/z = 355.1837 $[M + H]^+$. Elemental analysis = calculated: C, 74.55%; H, 7.68%; found: C, 74.16%; H, 7.60%.

Synthesis of (1*R*,3*S*,5*S*,7*R*)-8-([1,1′-biphenyl]-2-yl)-1,3,5,7-tetramethyl-2,4,6-trioxa-8-phospha-ada-mantane (ligand 3).[5h] In a glovebox, 1,3,5,7-tetramethyl-2,4,6-trioxa-8-phospha-adamantane (Cg-H, 0.10 g, 0.46 mmol), $Pd(PPh_3)_4$ (0.016 g, 0.014 mmol, 3 mol%), 2-bromo-1,1′-biphenyl (0.08 cm^3, 0.46 mmol), and K_2CO_3 (0.19 g, 1.40 mmol) were transferred in a flamed dried Schlenk tube containing degassed toluene (5.00 cm^3). The reaction mixture was evacuated and backfilled with argon (10 times) and refluxed (110 °C) for 24 h under argon. The reaction mixture was cooled to rt, diluted with degassed ethyl acetate (50 cm^3), and washed with (i) saturated and degassed ammonium chloride (10 cm^3 × 2), (ii) degassed water (10 cm^3), and (iii) degassed brine (10 cm^3). The resulting deep brown oil was purified by column chromatography on silica gel (5% v/v degassed ethyl acetate/hexane). The desired product was obtained as white crystals (0.13 g, 76%) which were 100% pure (pure based on NMR) in most cases. To improve purity where applicable, the solids were recrystallised in degassed ethyl acetate and degassed hexane (1 : 3). ^{1}H NMR (500 MHz, $CDCl_3$) δ = 8.37 (d, J = 7.0 Hz, 1H, ArH^1), 7.43–7.35 (m, 6H, $ArH_{(2,5,6)}$), 7.34–7.30 (m, 1H, $ArH_{(4)}$), 7.29–7.25 (m, 1H, $ArH_{(3)}$), 2.03 (m, 1H, $CgH_{(Dax)}$), 1.90 (m, 2H, $CgH_{(Deq)}$ and $CgH_{(Ceq)}$), 1.53 (d, $^3J_{P-H}$ = 12.4 Hz, 3H, $CgH_{(A2)}$), 1.44 (s, 3H, $CgH_{(B2)}$), 1.40 (d, J = 3.6 Hz, 1H, $CgH_{(Cax)}$), 1.33 (s, 3H, $CgH_{(B1)}$), 0.92 (d, $^3J_{P-H}$ = 11.9 Hz, 3H, $CgH_{(A1)}$). ^{13}C NMR (126 MHz, $CDCl_3$) δ = 151.06 (d, $^1J_{CP}$ = 28.6 Hz, $ArC_{(Ipso1)}$), 141.83 (d, $^2J_{CP}$ = 6.1 Hz, $ArC_{(Ipso2)}$), 133.83 (d, $^2J_{CP}$ = 3.1 Hz, $ArC_{(1)}$), 132.33 (d, $^3J_{CP}$ = 33.3 Hz, $ArC_{(Ipso3)}$), 131.01 (d, $^4J_{CP}$ = 4.8 Hz, $ArC_{(5)}$), 130.89 (d, $^4J_{CP}$ = 5.2 Hz, $ArC_{(3)}$), 129.11 ($ArC_{(2)}$), 127.56 ($ArC_{(6)}$), 127.05 (d, $^3J_{CP}$ = 4.5 Hz, $ArC_{(4)}$), 96.75 ($CgC_{(Q4)}$), 95.97 ($CgC_{(Q3)}$), 73.94 (d, $^1J_{CP}$ = 7.2 Hz, $CgC_{(Q1)}$), 73.79 (d, $^1J_{CP}$ = 21.6 Hz, $CgC_{(Q2)}$), 45.99 (d, $^2J_{CP}$ = 19.4 Hz, $CgC_{(D)}$), 36.04 ($CgC_{(C)}$), 28.10 ($CgC_{(B2)}$), 27.96 (d, $^2J_{CP}$ = 20.6 Hz, $CgC_{(A1)}$), 27.70 ($CgC_{(B1)}$), 26.78 (d, $^2J_{CP}$ = 11.4 Hz, $CgC_{(A2)}$). ^{31}P NMR (202 MHz, $CDCl_3$) δ = −39.06. HR-ESI-MS = calculated m/z = 369.1620 $[M + H]^+$, found m/z = 369.1624 $[M + H]^+$. Elemental analysis = calculated: C, 71.72%; H, 6.84%; found: C, 71.82%; H, 6.93%.

Synthesis of *N*,*N*-dimethyl-2′-((1*R*,3*S*,5*S*,7*R*)-1,3,5,7-tetramethyl-2,4,6-trioxa-8-phospha-adamantan-8-yl)[1,1′-biphenyl]-2-amine (ligand 4). In a glovebox, 1,3,5,7-tetramethyl-2,4,6-trioxa-8-phospha-adamantane (Cg-H, 0.5 g, 2.31 mmol), $Pd(PPh_3)_4$ (0.08 g, 0.069 mmol, 3 mol%), 2′-bromo-*N*,*N*-dimethyl-[1,1′-biphenyl]-2-amine (0.64 g, 2.31 mmol), and K_3PO_4 (1.47 g, 6.94 mmol) were transferred in a flamed dried Schlenk tube containing degassed toluene (5.00 cm^3). The reaction mixture was evacuated and backfilled with argon (10 times) and refluxed (110 °C) for 48 h under argon. The reaction mixture was cooled to rt, diluted with degassed ethyl acetate (150 cm^3), and washed with (i) saturated and degassed ammonium chloride (50 cm^3 × 2), (ii) degassed water (50 cm^3), and (iii) degassed brine (50 cm^3). The resulting deep brown oil was purified by column chromatography on silica gel (10% v/v degassed ethyl acetate/hexane). The desired product was obtained as white crystals (0.76 g, 80%) which were 100% pure (pure based on NMR) in most cases. To improve purity where applicable, the solids were recrystallised in degassed THF and degassed acetone (1 : 3). ^{1}H NMR (500 MHz, $CDCl_3$) δ = 8.28 (d, J = 7.8 Hz, 1H, $ArH_{(1)}$), 7.41 (t, J = 7.4 Hz, 1H, $ArH_{(3)}$), 7.33–7.24 (m, 3H, $ArH_{(2,4,7)}$), 7.09–7.04 (m, 1H, $ArH_{(5)}$), 7.00–6.94 (m, 2H, $ArH_{(6,\ 8)}$), 2.42 (s, 6H, NMe_2), 1.99–1.91 (m, 2H, $CgH_{(Ceq)}$, $CgH_{(Dax)}$), 1.85 (dd, J = 26.1, 13.0 Hz, 1H, $CgH_{(Deq)}$), 1.44–1.38 (m, 7H, $CgH_{(B2)}$, $CgH_{(A2)}$, $CgH_{(Cax)}$), 1.30 (s, 3H, $CgH_{(B1)}$), 0.86 (d, J = 11.9 Hz, 3H, $CgH_{(A1)}$). ^{13}C NMR (126 MHz, $CDCl_3$) δ = 151.34 (d, J = 2.4 Hz, $ArC_{(Ipso4)}$), 150.28 (d, J = 32.5 Hz, $ArC_{(Ipso1)}$), 135.22 (d, J = 6.0 Hz, $ArC_{(Ipso3)}$), 133.84 (d, J = 4.0 Hz, $ArC_{(1)}$), 133.57 ($ArC_{(Ipso2)}$), 131.89 ($ArC_{(5)}$), 130.66 (d, J = 6.4 Hz, $ArC_{(4)}$), 129.63 ($ArC_{(3)}$), 128.54 ($ArC_{(7)}$), 126.51 ($ArC_{(2)}$), 121.31 ($ArC_{(6)}$), 118.15 ($ArC_{(8)}$), 96.85 ($CgC_{(Q4)}$), 95.97 ($CgC_{(Q3)}$), 74.10 (d, J = 17.9 Hz, $CgC_{(Q2)}$), 73.95 (d, J = 1.4 Hz, $CgC_{(Q1)}$), 46.17 (d, J = 20.4 Hz, $CgC_{(D)}$), 42.90 (NMe_2), 36.26 ($CgC_{(C)}$), 28.18–27.97 ($CgC_{(B2)}$, $CgC_{(A1)}$), 27.78 ($CgC_{(B1)}$), 26.22 (d, J = 11.4 Hz, $CgC_{(A1)}$). ^{31}P NMR (202 MHz, $CDCl_3$) δ = −34.93. HR-ESI-MS = calculated m/z = 412.2042 $[M + H]^+$, found m/z = 412.2046 $[M + H]^+$.

General procedure for room temperature Suzuki–Miyaura

An oven-dried ace pressure tube was evacuated and backfilled with argon. $Pd(OAc)_2$ (0.01 mmol, 1 mol%) and ligand (0.02 mmol, 2 mol%), were added and the tube was evacuated and backfilled with argon. THF (2.00 mL), aryl halide (1 mmol), boronic acid (1.5 mmol), 2 M KOH dissolved in MeOH (3 mmol), and *n*-decane (0.5 mmol, internal standard), were added to the tube. The tube underwent a final evacuation/backfill cycle, sealed with a screw cap, and allowed to stir at room temperature (25 °C) for the specified times. Conversion, selectivity and GC yield were quantified from an aliquot (0.20 mL) of the reaction mixture using GC-FID. Upon completion, the GC sample was transferred back into the main reaction mixture, an aqueous work-up was performed (EtOAc : H_2O, 1 : 1). The organic layer was dried over $MgSO_4$, filtered through a cotton wool plug and concentrated on a rotary evaporator. The isolated yield was obtained by purification of the crude product through column chromatography using silica gel (EtOAc–hexane).

Characterisation data

4-Methyl-biphenyl.[11a] ^{1}H NMR (400 MHz, $CDCl_3$) δ = 7.66–7.61 (m, 2H), 7.55 (d, J = 8.2 Hz, 2H), 7.51–7.44 (m, 2H), 7.41–7.34 (m, 1H), 7.30 (d, J = 8.0 Hz, 2H), 2.45 (s, 3H). ^{13}C NMR (101 MHz, $CDCl_3$) δ = 141.24, 138.44, 137.09, 129.57, 128.80, 127.08, 127.06, 21.18.

3-Methyl-biphenyl.[11b] ^{1}H NMR (400 MHz, $CDCl_3$) δ = 7.62–7.57 (m, 2H), 7.46–7.38 (m, 4H), 7.37–7.30 (m, 2H), 7.17 (d, J = 7.5 Hz, 1H), 2.43 (s, 3H). ^{13}C NMR (101 MHz, $CDCl_3$) δ = 141.40, 141.27, 138.35, 128.72, 128.69, 128.02, 128.01, 127.21, 127.18, 124.30, 21.57.

2-Phenylnaphthalene.[11c] ^{1}H NMR (500 MHz, $CDCl_3$) δ = 8.09 (d, J = 0.6 Hz, 1H), 7.92 (dt, J = 8.8, 4.9 Hz, 3H), 7.81–7.75 (m, 3H), 7.56–7.49 (m, 4H), 7.45–7.39 (m, 1H). ^{13}C NMR (101 MHz, $CDCl_3$) δ = 141.21, 138.64, 133.77, 132.71, 128.94, 128.50, 128.29, 127.73, 127.51, 127.43, 126.36, 126.01, 125.89, 125.68.

2-Methoxy-6-phenylnaphthalene.[11c] ^{1}H NMR (500 MHz, $CDCl_3$) δ = 7.98 (s, 1H), 7.80 (dd, J = 8.3, 6.7 Hz, 2H), 7.74–7.69 (m, 3H), 7.48 (t, J = 7.7 Hz, 2H), 7.37 (t, J = 7.4 Hz, 1H), 7.21–7.15 (m, 2H), 3.94 (s, 3H). ^{13}C NMR (101 MHz, $CDCl_3$) δ = 157.81, 141.24, 136.42, 133.82, 129.75, 129.22, 128.86, 127.29, 127.26, 127.10, 126.07, 125.65, 119.19, 105.62, 55.36.

3,5-Dimethyl-1,1′-biphenyl.[11b] ^{1}H NMR (500 MHz, $CDCl_3$) δ = 7.61–7.57 (m, 2H), 7.45–7.41 (m, 2H), 7.34 (dd, J = 13.2, 5.9 Hz, 1H), 7.22 (s, 2H), 7.01 (s, 1H), 2.39 (s, 6H). ^{13}C NMR (101 MHz, $CDCl_3$) δ = 141.51, 141.30, 138.27, 128.92, 128.78, 128.66, 127.28, 127.22, 127.20, 127.10, 125.14, 21.44.

2,4-Dimethyl-1,1′-biphenyl.[11d] ^{1}H NMR (500 MHz, $CDCl_3$) δ = 7.46 (dd, J = 10.4, 4.4 Hz, 2H), 7.41–7.35 (m, 3H), 7.20 (d, J = 7.7 Hz, 1H), 7.16 (s, 1H), 7.12 (d, J = 7.7 Hz, 1H), 2.43 (s, 3H), 2.31 (s, 3H). ^{13}C NMR (101 MHz, $CDCl_3$) δ = 142.04, 139.20, 136.94, 135.21, 131.17, 129.84, 129.37, 128.84, 128.11, 127.25, 126.67, 126.57, 21.13, 20.46.

2,4,6-Trimethyl-1,1′-biphenyl.[7n] ^{1}H NMR (400 MHz, $CDCl_3$) δ = 7.48 (t, J = 7.4 Hz, 2H), 7.40 (d, J = 7.4 Hz, 1H), 7.22 (t, J = 6.3 Hz, 2H), 7.03 (s, 2H), 2.41 (s, 3H), 2.09 (s, 6H). ^{13}C NMR (126 MHz, $CDCl_3$) δ = 141.19, 139.16, 136.64, 136.06, 129.39, 128.47, 128.16, 126.61, 21.14, 20.86.

4-Methoxy-biphenyl.[11a] ^{1}H NMR (400 MHz, $CDCl_3$) δ = 7.61–7.53 (m, 4H), 7.44 (dd, J = 10.5, 4.8 Hz, 2H), 7.32 (dd, J = 10.5, 4.2 Hz, 1H), 7.04–6.97 (m, 2H), 3.86 (s, 3H). ^{13}C NMR (101 MHz, $CDCl_3$) δ = 159.20, 140.88, 133.82, 128.78, 128.21, 126.79, 126.71, 114.26, 55.37.

2-Methoxy-biphenyl.[11b] ^{1}H NMR (400 MHz, $CDCl_3$) δ = 7.56 (dd, J = 5.3, 3.1 Hz, 2H), 7.45–7.40 (m, 2H), 7.34 (ddd, J = 7.3, 4.3, 1.4 Hz, 3H), 7.08–6.98 (m, 2H), 3.82 (s, 3H). ^{13}C NMR (101 MHz, $CDCl_3$) δ = 156.51, 138.59, 130.93, 130.78, 129.59, 128.80, 128.65, 128.02, 127.21, 126.95, 120.87, 111.29, 55.58.

2,6-Dimethoxy-1′-biphenyl.[11a] ^{1}H NMR (500 MHz, $CDCl_3$) δ = 7.46–7.29 (m, 3H), 6.68 (d, J = 8.4 Hz, 1H), 3.75 (s, 3H). ^{13}C NMR (101 MHz, $CDCl_3$) δ = 157.74, 134.21, 130.95, 128.69, 127.71, 126.81, 119.65, 104.29, 55.96.

2,4′-Dimethyl-1,1′-biphenyl.[11e] ^{1}H NMR (500 MHz, $CDCl_3$) δ = 7.34–7.27 (m, 3H), 2.48 (s, 1H), 2.35 (s, 1H). ^{13}C NMR (126 MHz, $CDCl_3$) δ = 141.94, 139.10, 136.37, 135.41, 130.29, 129.87, 129.10, 128.79, 127.08, 125.75, 21.18, 20.51.

2,4′,6-Trimethyl-1,1′-biphenyl.[11e] ^{1}H NMR (500 MHz, $CDCl_3$) δ = 7.23 (d, J = 7.6 Hz, 2H), 7.17–7.13 (m, 1H), 7.10 (d, J = 7.3 Hz, 2H), 7.04 (d, J = 7.7 Hz, 2H), 2.41 (s, 3H), 2.04 (s, 6H). ^{13}C NMR (126 MHz, $CDCl_3$) δ = 141.86, 138.06, 136.22, 136.06, 129.11, 128.90, 127.24, 126.87, 21.23, 20.87.

3-Phenyl-pyridine.[11f] ^{1}H NMR (500 MHz, $CDCl_3$) δ = 8.82 (s, 1H), 8.55 (d, J = 4.7 Hz, 1H), 7.81 (d, J = 7.8 Hz, 1H), 7.53 (d, J = 8.0 Hz, 2H), 7.43 (t, J = 7.6 Hz, 2H), 7.36 (t, J = 7.0 Hz, 1H), 7.30 (dd, J = 7.6, 4.9 Hz, 1H). ^{13}C NMR (126 MHz, $CDCl_3$) δ = 148.47, 148.33, 137.83, 137.82, 136.58, 134.25, 129.05, 128.07, 127.12, 123.49.

2-Phenyl-pyridine.[11g] ^{1}H NMR (500 MHz, $CDCl_3$) δ = 8.68 (d, J = 4.3 Hz, 1H), 7.99 (d, J = 7.7 Hz, 2H), 7.70 (s, 2H), 7.46 (t, J = 7.5 Hz, 2H), 7.40 (t, J = 7.2 Hz, 1H), 7.19 (s, 1H). ^{13}C NMR (126 MHz, $CDCl_3$) δ = 157.49, 149.69, 139.45, 136.71, 128.96, 128.75, 126.93, 122.08, 120.53.

2-Phenyl-quinoline.[11h] ^{1}H NMR (500 MHz, $CDCl_3$) δ = 8.23–8.14 (m, 4H), 7.84 (d, J = 8.6 Hz, 1H), 7.79 (d, J = 8.1 Hz, 1H), 7.73 (dd, J = 8.1, 7.2 Hz, 1H), 7.56–7.49 (m, 3H), 7.48 (dd, J = 10.8, 3.7 Hz, 1H). ^{13}C NMR (126 MHz, $CDCl_3$) δ = 157.35, 148.36, 139.72, 136.77, 129.81, 129.67, 129.36, 128.87, 127.63, 127.50, 127.24, 126.30, 118.98.

2-Phenyl-thiophene.[11f] ^{1}H NMR (500 MHz, $CDCl_3$) δ = 7.42 (d, J = 5.6 Hz, 1H), 7.34 (bs, 1H), 7.28–7.22 (m, 3H), 7.11–7.07 (m, 2H), 2.44 (s, 3H). ^{13}C NMR (101 MHz, $CDCl_3$) δ = 143.16, 136.16, 134.22, 130.79, 130.54, 127.85, 127.15, 126.45, 125.96, 125.18, 21.25.

3-(*o*-Tolyl)pyridine.[11i] ^{1}H NMR (500 MHz, $CDCl_3$) δ = 8.62–8.55 (m, 2H), 7.66–7.61 (m, 1H), 7.33 (m, 1H), 7.30–7.24 (m, 3H), 7.20 (d, J = 7.2 Hz, 1H), 2.26 (s, 3H). ^{13}C NMR (101 MHz, $CDCl_3$) δ = 149.93, 148.09, 138.09, 137.49, 136.50, 135.60, 130.57, 129.87, 128.12, 126.08, 123.02, 20.35.

2-(*o*-Tolyl)-thiophene.[11j] ^{1}H NMR (400 MHz, $CDCl_3$) δ = 7.48–7.44 (m, 1H), 7.37 (d, J = 5.0 Hz, 1H), 7.32–7.26 (m, 3H), 7.13 (m, 2H), 2.48 (s, 3H). ^{13}C NMR (101 MHz, $CDCl_3$) δ = 143.16, 136.16, 134.22, 130.79, 130.54, 127.85, 127.15, 126.45, 125.96, 125.18, 21.25.

2-(2,6-Dimethylphenyl)pyridine.[11k] ^{1}H NMR (500 MHz, $CDCl_3$) δ = 8.75–8.64 (m, 1H), 7.73 (t, J = 7.6 Hz, 1H), 7.25–7.14

(m, 3H), 7.08 (d, J = 7.5 Hz, 2H), 2.02 (s, 6H). ^{13}C NMR (101 MHz, $CDCl_3$) δ = 159.94, 149.75, 140.52, 136.31, 135.79, 127.88, 127.55, 124.46, 121.69, 20.26.

3-(2,6-Dimethylphenyl)pyridine.[11l] ^{1}H NMR (400 MHz, $CDCl_3$) δ = 8.59 (dd, J = 4.9, 1.7 Hz, 1H), 8.43 (dd, J = 2.2, 0.9 Hz, 1H), 7.52–7.47 (m, 1H), 7.36 (m, 1H), 7.19 (dd, J = 8.5, 6.5 Hz, 1H), 7.13–7.10 (m, 2H), 2.02 (s, 6H). ^{13}C NMR (101 MHz, $CDCl_3$) δ = 150.04, 148.11, 137.85, 136.78, 136.69, 136.31, 127.89, 127.58, 123.41, 20.91.

2-(2,6-Dimethylphenyl)-thiophene.[11l] ^{1}H NMR (400 MHz, $CDCl_3$) δ = 7.40 (d, J = 5.1 Hz, 1H), 7.24–7.19 (m, 1H), 7.14 (d, J = 7.7 Hz, 3H), 6.86 (d, J = 2.8 Hz, 1H), 2.19 (s, 6H). ^{13}C NMR (101 MHz, $CDCl_3$) δ = 141.40, 138.51, 134.13, 128.15, 127.33, 127.13, 126.33, 125.36, 20.88.

Conflicts of interest

There are no conflicts to declare.

Acknowledgements

We are grateful for financial support from Research Centre for Synthesis and Catalysis (University of Johannesburg) and Sasol (Pty) Ltd. We thank Mr Mutshinyalo Nwamadi (NMR) as well as Dr Banele Vatsha and Dr Frederick Malan for assistance with X-Ray crystallography. The authors also thank Sasol Research & Technology (South Africa) for providing secondary phosphines phobane-H and Cg-H. Stellenbosch University Central Analytical Facilities is acknowledged for mass spectrometry analysis.

Notes and references

1 (*a*) T. J. Colacot, *New Trends in Cross-Coupling Theory and Applications*, The Royal Society of Chemistry, Cambridge, 2015; (*b*) P. G. Gildner and T. J. Colacot, *Organometallics*, 2015, **34**, 5497–5508.

2 (*a*) A. Taheri Kal Koshvandi, M. M. Heravi and T. Momeni, *Appl. Organomet. Chem.*, 2018, **32**, 1–59; (*b*) M. A. Selepe and F. R. Van Heerden, *Molecules*, 2013, **18**, 4739–4765.

3 (*a*) R. Bernini, S. Cacchi, I. De Salve and G. Fabrizi, *Tetrahedron Lett.*, 2007, **48**, 4973–4976; (*b*) S. Xu, E. H. Kim, A. Wei and E. Negishi, *Sci. Technol. Adv. Mater.*, 2014, **15**, 1–23; (*c*) B. J. Reizman, Y. M. Wang, S. L. Buchwald and K. F. Jensen, *React. Chem. Eng.*, 2016, **1**, 658–666; (*d*) K. L. Billingsley, K. W. Anderson and S. L. Buchwald, *Angew. Chem., Int. Ed.*, 2006, **45**, 3484–3488; (*e*) R. Martin and S. L. Buchwald, *Acc. Chem. Res.*, 2008, **41**, 1461–1473; (*f*) X. Shen, G. O. Jones, D. A. Watson, B. Bhayana and S. L. Buchwald, *J. Am. Chem. Soc.*, 2010, **132**, 11278–11287.

4 (*a*) J. P. Wolfe, R. A. Singer, B. H. Yang and S. L. Buchwald, *J. Am. Chem. Soc.*, 1999, **121**, 9550–9561; (*b*) J. P. Wolfe and S. L. Buchwald, *Angew. Chem., Int. Ed.*, 1999, **38**, 2413–2416; (*c*) S. D. Walker, T. E. Barder, J. R. Martinelli and S. L. Buchwald, *Angew. Chem., Int. Ed.*, 2004, **43**, 1871–1876; (*d*) H. Ji, L. Y. Wu, J. H. Cai, G. R. Li, N. N. Gan and Z. H. Wang, *RSC Adv.*, 2018, **8**, 13643–13648; (*e*) T. Willemse, W. Schepens, H. W. T. Van Vlijmen, B. U. W. Maes and S. Ballet, *Catalysts*, 2017, **7**, 1–32; (*f*) B. Bhayana, B. P. Fors and S. L. Buchwald, *Org. Lett.*, 2009, **11**, 3954–3957; (*g*) S. L. Buchwald, H. N. Nguyen and X. Huang, *J. Am. Chem. Soc.*, 2003, **125**, 11818–11819; (*h*) K. H. Chung, C. M. So, S. M. Wong, C. H. Luk, Z. Zhou, C. P. Lau and F. Y. Kwong, *Chem. Commun.*, 2012, **48**, 1967; (*i*) W. Shu, L. Pellegatti, M. A. Oberli and S. L. Buchwald, *Angew. Chem., Int. Ed.*, 2011, **50**, 10665–10669; (*j*) C. Len, S. Bruniaux, F. Delbecq and V. Parmar, *Catalysts*, 2017, **7**, 146; (*k*) T. Seo, T. Ishiyama, K. Kubota and H. Ito, *Chem. Sci.*, 2019, **10**, 8202–8210; (*l*) K. Kubota and H. Ito, *Trends Chem.*, 2020, 1–16; (*m*) D. W. Old, J. P. Wolfe and S. L. Buchwald, *J. Am. Chem. Soc.*, 1998, **120**, 9722–9723; (*n*) T. E. Barder and S. L. Buchwald, *J. Am. Chem. Soc.*, 2007, **129**, 5096–5101.

5 (*a*) R. A. Baber, M. L. Clarke, K. M. Heslop, A. C. Marr, A. G. Orpen, P. G. Pringle, A. Ward and D. E. Zambrano-Williams, *J. Chem. Soc., Dalton Trans.*, 2005, **6**, 1079–1085; (*b*) T. Brenstrum, D. A. Gerristma, G. M. Adjabeng, C. S. Frampton, J. Britten, A. J. Robertson, J. McNulty and A. Capretta, *J. Org. Chem.*, 2004, **69**, 7635–7639; (*c*) M. F. Haddow, J. Jaltai, M. Hanton, P. G. Pringle, L. E. Rush, H. A. Sparkes and C. H. Woodall, *J. Chem. Soc., Dalton Trans.*, 2016, **45**, 2294–2307; (*d*) M. Carreira, M. Charernsuk, M. Eberhard, N. Fey, R. Van Ginkel, A. Hamilton, W. P. Mul, A. G. Orpen, H. Phetmung and P. G. Pringle, *J. Am. Chem. Soc.*, 2009, **131**, 3078–3092; (*e*) P. N. Bungu and S. Otto, *J. Chem. Soc., Dalton Trans.*, 2007, **2**, 2876–2884; (*f*) G. Adjabeng, T. Brenstrum, J. Wilson, C. Frampton, A. Robertson, J. Hillhouse, J. McNulty and A. Capretta, *Org. Lett.*, 2003, **5**, 953–955; (*g*) C. M. Le, X. Hou, T. Sperger, F. Schoenebeck and M. Lautens, *Angew. Chem., Int. Ed.*, 2015, **54**, 15897–15900; (*h*) S. Shekhar, T. S. Franczyk, D. M. Barnes, T. B. Dunn, A. R. Haight and V. S. Chan, *US Pat.*, 20160263566A1, AbbVie Inc., 2016.

6 (*a*) H. Shet, U. Parmar, S. Bhilare and A. R. Kapdi, *Org. Chem. Front.*, 2021, **1**, 1–58; (*b*) Y. Zhao, H. van Nguyen, L. Male, P. Craven, B. R. Buckley and J. S. Fossey, *Organometallics*, 2018, **37**, 4224–4241; (*c*) A. Brand and W. Uhl, *Chem.–Eur. J.*, 2019, **25**, 1391–1404; (*d*) C. M. Donahue, S. P. McCollom, C. M. Forrest, A. V. Blake, B. J. Bellott, J. M. Keith and S. R. Daly, *Inorg. Chem.*, 2015, **54**, 5646–5659; (*e*) S. Hanf, A. L. Colebatch, P. Stehr, R. García-Rodríguez, E. Hey-Hawkins and D. S. Wright, *Dalton Trans.*, 2020, **49**, 5312–5322; (*f*) A. J. Kendall, L. N. Zakharov and D. R. Tyler, *Inorg. Chem.*, 2016, **55**, 3079–3090; (*g*) P. N. Bungu and S. Otto, *J. Organomet. Chem.*, 2007, **692**, 3370; (*h*) A. L. Rheingold, *CSD Commun.*, 2016, **1**, 1; (*i*) T. Ikawa, T. E. Barder, M. R. Biscoe and S. L. Buchwald, *J. Am. Chem. Soc.*, 2007, **129**, 13001–13007.

7 (*a*) I. Maluenda and O. Navarro, *Molecules*, 2015, **20**, 7528–7557; (*b*) A. F. Littke and G. C. Fu, *Angew. Chem., Int. Ed.*, 1999, **37**, 3387–3388; (*c*) J. El-maiss, T. Mohy, E. Dine, C. Lu, I. Karam, A. Kanj, K. Polychronopoulou and J. Shaya, *Catalysts*, 2020, **10**, 296; (*d*) S. Kotha, K. Lahiri and D. Kashinath, *Tetrahedron*, 2002, **58**, 9633–9695; (*e*) M. A. Selepe and F. R. Van Heerden, *Molecules*, 2013, **18**,

4739–4765; (*f*) G. W. Kabalka, V. Namboodiri and L. Wang, *Chem. Commun.*, 2001, **1**, 775; (*g*) C. Amatore, A. Jutand and G. Leduc, *Angew. Chem., Int. Ed.*, 2012, **51**, 1379–1382; (*h*) J. H. Li, C. L. Deng and Y. X. Xie, *Synth. Commun.*, 2007, **37**, 2433–2448; (*i*) R. Rabie, M. M. Hammouda and K. M. Elattar, *Res. Chem. Intermed.*, 2017, **43**, 1979–2015; (*j*) A. R. Hajipour, K. Karami and G. Tavakoli, *Appl. Organomet. Chem.*, 2012, **26**, 401–405; (*k*) T. E. Barder, S. D. Walker, J. R. Martinelli and S. L. Buchwald, *J. Am. Chem. Soc.*, 2005, **127**, 4685–4696; (*l*) D. Schaarschmidt and H. Lang, *Eur. J. Inorg. Chem.*, 2010, **1**, 4811–4821; (*m*) M. C. Lipke, R. A. Woloszynek, L. Ma and J. D. Protasiewicz, *Organometallics*, 2009, **28**, 188–196; (*n*) B. Lin, Z. Liu, M. Liu, C. Pan, J. Ding, H. Wu and J. Cheng, *Catal. Commun.*, 2007, **8**, 2150–2152; (*o*) G. Cao, H. Q. Yang, B. T. Luo and F. S. Liu, *J. Organomet. Chem.*, 2013, **745–746**, 158–165; (*p*) S. Tröndle, A. C. Tagne Kuate, M. Freytag, P. G. Jones and M. Tamm, *Eur. J. Inorg. Chem.*, 2017, **2017**, 5588–5597; (*q*) Z. L. Niemeyer, A. Milo, D. P. Hickey and M. S. Sigman, *Nat. Chem.*, 2016, **8**, 610–617, and references therein. (*r*) J. Jover and J. Cirera, *J. Chem. Soc., Dalton Trans.*, 2019, **48**, 15036–15048; (*s*) H. Clavier and S. P. Nolan, *Chem. Commun.*, 2010, **46**, 841–861.

8 (*a*) A. A. Altaf, A. Shahzad, Z. Gul, N. Rasool, A. Badshah, B. Lal and E. Khan, *J. Drug Des. Med. Chem.*, 2015, **1**, 1–11; (*b*) G. Clavé, F. Pelissier, S. Campidelli and C. Grison, *Green Chem.*, 2017, **19**, 4093–4103; (*c*) G. Yang, C. Sau, W. Lai, J. Cichon and W. Li, *Curr. Top. Med. Chem.*, 2015, **344**, 1173–1178; (*d*) H. W. Lee, C. M. So, O. Y. Yuen, W. T. Wong and F. Y. Kwong, *Org. Chem. Front.*, 2020, **7**, 926–932; (*e*) T. Itoh and T. Mase, *Tetrahedron Lett.*, 2005, **46**, 3573–3577; (*f*) S. Wagaw and S. L. Buchwald, *J. Org. Chem.*, 1996, **61**, 7240–7241.

9 (*a*) G. C. Fu, *Acc. Chem. Res.*, 2008, **41**, 1555; (*b*) D. Roy and Y. Uozumi, *Adv. Synth. Catal.*, 2018, **360**, 602–625; (*c*) S. E. Hooshmand, B. Heidari, R. Sedghi and R. S. Varma, *Green Chem.*, 2019, **21**, 381–405; (*d*) T. Tagata and M. Nishida, *J. Org. Chem.*, 2003, **68**, 9412–9415.

10 (*a*) Rigaku Oxford Diffraction, *CrysAlisPro Softw. Syst.*2018; (*b*) W. SAINT, *Data Reduction Software, Version 6.45*, Bruker AXS Inc., Madison, 2003; (*c*) W. SADABS, *Version 2.05*, Bruker AXS Inc., Madison, 2002; (*d*) R. H. Blessing, *Acta Crystallogr., Sect. A: Found. Crystallogr.*, 1995, **51**, 33–38; (*e*) G. M. Sheldrick, *Acta Crystallogr., Sect. A: Found. Crystallogr.*, 2008, **64**, 112–122; (*f*) G. M. Sheldrick, *Acta Crystallogr., Sect. A: Found. Crystallogr.*, 2015, **71**, 3–8; (*g*) O. V. Dolomanov, L. J. Bourhis, R. J. Gildea, J. A. K. Howard and H. Puschmann, *J. Appl. Crystallogr.*, 2009, **42**, 339–341.

11 (*a*) T. Zhou, P. P. Xie, C. L. Ji, X. Hong and M. Szostak, *Org. Lett.*, 2020, **22**, 6434–6440; (*b*) G. Rizzo, G. Albano, M. Lo Presti, A. Milella, F. G. Omenetto and G. M. Farinola, *Eur. J. Org. Chem.*, 2020, 6992–6996; (*c*) H. Chen, Z. Huang, X. Hu, G. Tang, P. Xu, Y. Zhao and C. Cheng, *J. Org. Chem.*, 2011, **76**, 2338–2344; (*d*) P. Pattanayak, S. P. Parua and S. Chattopadhyay, *Polyhedron*, 2019, **157**, 410–415; (*e*) P. Y. Choy, O. Y. Yuen, M. P. Leung, W. Kin and F. Y. Kwong, *Eur. J. Org. Chem.*, 2020, **1**, 2846–2853; (*f*) H. Li, L. Zhao, Y. Liu, X. Zhang, W. Li, L. Jing, J. Huang and W. Wang, *Chin. J. Org. Chem.*, 2019, **39**, 3207–3214; (*g*) B. Lai, M. Ye, P. Liu, M. Li, R. Bai and Y. Gu, *Beilstein J. Org. Chem.*, 2020, **16**, 2888–2902; (*h*) X. Chen, J. Chen, Z. Bao, Q. Yang, Y. Yang, Q. Ren and Z. Zhang, *Chin. J. Org. Chem.*, 2019, **39**, 1681–1687; (*i*) L. Liu, K. Zhao, W. Li, M. Liu, Y. Chen and Y. Dong, *Appl. Organomet. Chem.*, 2019, **33**, 1–5; (*j*) M. T. Chen, Y. H. Lin and K. H. Jian, *Appl. Organomet. Chem.*, 2020, **34**, 1–11; (*k*) S. Ni, M. Hribersek, S. K. Baddigam, F. J. L. Ingner, A. Orthaber, P. J. Gates and L. T. Pilarski, *Angew. Chem., Int. Ed.*, 2021, **60**, 6660–6666; (*l*) D. D. Lu, X. X. He and F. S. Liu, *J. Org. Chem.*, 2017, **82**, 10898–10911.